



## A New Fuzzy Sliding Mode Controller for 2-DOF Aero System with Pitch Disturbance

Gaurav Kumawat\* and Niraj Kumar Goswami  
School of Automation, Banasthali Vidyapith, Tonk, Rajasthan, India

Jayashri Vajpai  
Department of Electrical Engineering, MBM University, Jodhpur, Rajasthan, India

\* Corresponding author. E-mail: gauravkumawat@banasthali.in DOI: 10.14416/j.asep.2025.07.013  
Received: 10 March 2025; Revised: 19 May 2025; Accepted: 17 June 2025; Published online: 24 July 2025  
© 2025 King Mongkut's University of Technology North Bangkok. All Rights Reserved.

### Abstract

The two-degree-of-freedom aero flight control simulator is a nonlinear, unstable, and multi-input multi-output system with gravitational disturbance in its pitch dynamics. Its attitude control is a challenging task with linear controllers. The fuzzy controller by parallel distributed compensation uses a combination of linear controllers. It is a simple method, but exhibits poor tracking performance under disturbance. This study presents a design of a fixed structure fuzzy sliding mode controller to track the desired trajectory for this system. A sliding mode controller is combined with the fuzzy controller using an integral sliding surface to overcome gravitational disturbance and track the attitude. Lyapunov's method verifies the stability of the closed-loop system. To validate the proposed design, numerical simulations are carried out and compared with existing methods. The tracking responses of yaw and pitch point out fast convergence of error with minimum settling time in the presence of matched disturbances.

**Keywords:** 2-DOF Aero system, Fuzzy controller, Fuzzy sliding mode controller, T-S fuzzy model

### 1 Introduction

In recent years, helicopter control system design has emerged as a prominent study area, owing to its extensive applications in military and civilian domains for supply, rescue, search missions, and surveillance [1], [2]. The helicopters are preferred over fixed-wing aircraft for their Vertical Take-Off and Landing (VTOL) capabilities, which makes them superior for hover and maneuverability. However, the helicopter has nonlinear [3], under-actuated, coupled [4], and uncertain [5] dynamics combined with environmental conditions, wind speed, and pressure pose a challenge to ensure stability and tracking of the reference trajectory. The Two Degrees Of Freedom (2-DOF) Quanser aero serves as a testbed for the investigation of control algorithms for helicopters.

Several control algorithms have been developed by many researchers to stabilize and control helicopters. This includes some linear controllers, including Linear Quadratic Regulator (LQR) [6],

Proportional Integral Derivative Controller (PID) [1], some intelligent controllers, including Fuzzy Controller (FC) [2], neuro-fuzzy controller [7], some advance controllers, including the adaptive backstepping controller (ABS) [3], Sliding Mode Controller (SMC) [4], etc. The PID [1] and LQR [6] are some classical linear controllers that are extensively used to control nonlinear systems. They can be designed by linearizing the nonlinear system around some operating point. These controllers perform well around the neighborhood of those operating points; beyond their performance of linear controllers degrades drastically. Their performance is also affected by unmodelled dynamics, time-varying parameters, and disturbance, so nonlinear controllers (e.g. FC, SMC, etc.) worked well for larger operating ranges and robustness against uncertainty and disturbance.

A fuzzy controller [2] has been designed using a Mamdani inference system with forty-nine rules. This controller was designed using an input-output

relationship. [3] designed an adaptive backstepping controller for tracking of desired trajectory in the presence of unknown parameters. SMC has shown excellent tracking ability and robustness against parametric uncertainty and external disturbance [8]–[10]. Adaptive backstepping has some limitations e.g. over-parameterization of unknown parameters, and higher order derivatives of virtual control, which can increase the complexity of hardware implementation. [4] designed a conventional SMC with a PD sliding surface, but it suffers from chattering in the controller's output and state of the system due to the discontinuous switching control part, so a saturation function was used to minimize chattering. [5] designed a novel sliding mode controller that has state-dependent gain and a combined twisting algorithm with sliding mode control to eliminate chattering and saturation of input voltages of the motors of the system. The adaptive sliding mode controller uses time-varying switching gain to reduce chattering in the control law. This adaptive gain [11], [12] is designed by an integral law, which can cause an overestimation of switching gain and slower transient response. [7] used an adaptive neural fuzzy inference system to optimize the fuzzy rule base using a neural network. [13] proposed a novel fractional order-based fuzzy model and sliding mode control for unidentified limits of parametric uncertainty. The actor-critic algorithm was employed along with online fractional order Reinforcement Learning (RFL) for the approximation of equivalent and switching control of SMC and the value function of RFL. [14] designed an adaptive backstepping control law for tracking the desired trajectory in a prescribed time while parametric uncertainty was present in the aero system. [15] proposed adaptive backstepping controller for a communication network system where both input and states are quantized. The limitation of communication networks was addressed in this work. [16] designed a multi-input multi-output PID controller for uncertain cross-coupled gains of the aero system. [17] designed an online Adaptive Neural Network Fuzzy Inference System (ANFIS) to tune the fuzzy controller to adapt to any change in parameters. [18] designed Uncertainty and Disturbance Estimator (UDE) with adaptive gain that works better than high-gain UDE. [19] proposed adaptive neural network controller to compensate for uncertainty and input saturation. A disturbance observer is also employed to observe disturbances and correct the neural network error.

The linear state feedback controllers provide a simple and easy approach to designing a controller for

the aero system. A reduced and full-order state observer [20] was designed using the linearized model of the aero system for an optimal LQR controller. [21]–[23] designed state feedback controllers for helicopters, considering the linearized model of the system. [21], [22] used two additional states, integration of outputs to improve steady-state error. [24] used a nonlinear feedforward control along with LQR and PID to compensate for the gravitational disturbance present in pitch dynamics for tracking performance improvement. This gravitational disturbance is a bounded and state-dependent disturbance that always has a nonzero value. [20]–[24] designed controllers for the linearized model of the aero system, neglecting nonlinearity, uncertainty, and disturbance as zero, which doesn't reflect the real behavior of the system. In the real world, these nonlinearities, disturbances, and uncertainty are always present in the system and should be considered for accurate control.

The Takagi-Sugeno (T-S) fuzzy model is a powerful method to express a wide variety of nonlinear systems by fuzzy rules containing the linear sub-systems. This enables us to use linear models for a wide operating range. The fuzzy model contains fuzzy propositions in the antecedent part, but the consequent part contains a local linearized sub-system of a nonlinear system. The Parallel distributed compensation (PDC) [25] approach is a T-S fuzzy model-based design approach for designing the fuzzy controller. In this approach, the linear subsystem of this model is replaced by a state feedback controller, and the whole model remains the same. These fuzzy controllers have excellent stabilization capabilities but lack tracking performance.

In this paper, the T-S fuzzy model of the 2-DOF aero system has been constructed to design a fuzzy controller by employing a set of linear controllers for a broad operating range. This fuzzy controller features a simple design structure due to a set of state feedback controllers, but its performance degrades because of gravitational pitch disturbance. The state feedback controller forces the system states to converge to zero as time approaches infinity. This gravitational pitch disturbance is a cosine function of the pitch angle; as the pitch angle converges to zero, the disturbance becomes constant, which is not eliminated by the state feedback controller law. Therefore, the sliding mode controller is combined with the fuzzy controller to provide robustness against this gravitational disturbance. The integral sliding surface offers a method to blend fuzzy and sliding mode controllers.

The equivalent control law, which is essential for sliding mode, is designed by the fuzzy controller, and the discontinuous control law will reject the gravitational disturbance. This robust controller is suitable for a larger operating range and can deliver faster convergence of tracking errors. Lyapunov’s method was employed to demonstrate the stability of the closed-loop system and derive the new Fuzzy Sliding Mode Controller (FSMC) law. The other FSMC was designed for fuzzy sliding surface [26], and fuzzy switching gain [27], which not only improves the performance but also alters the properties of SMC i.e., increase in reaching time, and convergence time. The proposed FSMC uses FC but keeps the properties of SMC intact. This is the novelty of the proposed controller.

## 2 Materials and Methods

### 2.1 Dynamic model of 2-DOF AERO

The 2-DOF aero system is a simplified model of a helicopter that has two identical rotors, resembling the main and tail rotors. The horizontally placed main rotor is powered by a DC motor and produces a torque about the pitch axis to attain the pitch angle. The aerodynamic drag of this rotor also causes the yaw angle. The vertically placed tail rotor is also powered by a DC motor, which produces a torque about the yaw axis to attain the yaw angle, and it also causes the pitch angle due to aerodynamic drag. The voltages of vertical and horizontal motors are the input; yaw and pitch angles are the outputs of this system. The yaw angle can vary all around the yaw axis at 360° in both clockwise and anticlockwise directions.

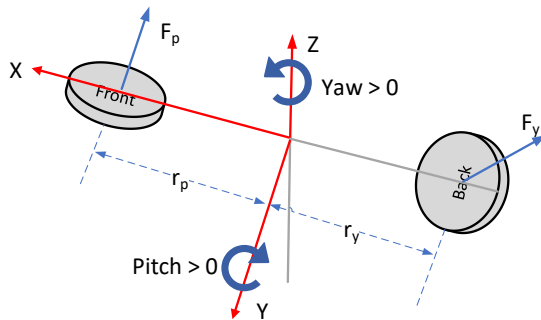


Figure 1: Free body diagram of 2-DOF Aero.

So, this system has two degrees of freedom, i.e., pitch and yaw. In this paper, both pitch and yaw

angular positions have been considered for trajectory tracking. The free body diagram of the 2-DOF aero system for understanding forces and angular displacement is given in Figure 1.

The equation of motion for the system under consideration is given in Equation (1)

$$\begin{aligned} \ddot{\theta} &= \frac{1}{(J_p + ml^2)} [K_{pp}V_p + K_{yp}V_y - B_p\dot{\theta} \\ &\quad - ml^2 \cos \theta \sin \theta \dot{\psi}^2 - mgl \cos \theta] \\ \ddot{\psi} &= \frac{1}{(J_y + ml^2 \cos^2 \theta)} [K_{yp}V_p + K_{yy}V_y - B_y\dot{\psi} + \\ &\quad 2ml^2 \cos \theta \sin \theta \dot{\theta} \dot{\psi}] \end{aligned} \quad (1)$$

Where  $\theta$  stands for pitch angle,  $\psi$  for yaw angle,  $V_p$  for the input voltage of the pitch motor,  $V_y$  for the input voltage of the yaw motor,  $B_y$  and  $B_p$  for viscous friction coefficients;  $J_y$  and  $J_p$  for the moments of inertia about the yaw and pitch axes, respectively and  $K_{pp}$ ,  $K_{py}$ ,  $K_{yp}$  and  $K_{yy}$  for thrust torque constants.

The state vector is  $x = [\theta(t), \psi(t), \dot{\theta}(t), \dot{\psi}(t)]^T \in R^4$ , the input vector is  $u = [V_p \ V_y]^T \in R^2$  and the output vector is  $y = [y_1 \ y_2]^T = [\theta(t) \ \psi(t)]^T \in R^2$ . The state space model of 2-DOF aero flight control simulator Equation (1) is given in Equation (2), as:

$$\dot{x} = f(x) + G(x)u \quad (2)$$

Where,  $f(x) = [x_3 \ x_4 \ f_1 \ f_2]^T \in R^4$ , is a vector of nonlinear functions of states,  $G(x) = [0_{2 \times 2}; g_{11}, g_{12}; g_{21}, g_{22}] \in R^{2 \times 2}$ , is a nonlinear input gain matrix.

$$\begin{aligned} f_1 &= \frac{-B_p x_3 - ml^2 \cos x_1 \sin x_1 x_4^2 - mgl \cos x_1}{J_p + ml^2}, \\ f_2 &= \frac{-B_y x_4 + 2ml^2 \cos x_1 \sin x_1 x_3 x_4}{J_y + ml^2 \cos^2 x_1}, \\ g_{11} &= \frac{K_{pp}}{J_p + ml^2}, \\ g_{12} &= \frac{K_{yp}}{J_p + ml^2}, \\ g_{21} &= \frac{K_{yp}}{J_y + ml^2 \cos^2 x_1}, \\ g_{22} &= \frac{K_{yy}}{J_y + ml^2 \cos^2 x_1}. \end{aligned}$$

The state space model of the system is designed on MATLAB Simulink to evaluate the performance of the designed controllers. The system parameters of the 2-DOF aero system are given in Table 1.

**Table 1:** Parameters of 2-DOF Aero system.

Parameter	Description	Value
$J_p$	Moment of inertia	0.0219 $Kgm^2$
$J_y$	Moment of inertia	0.022 $Kgm^2$
$B_p$	Viscus friction coefficient	0.00711 $Vs/rad$
$B_y$	Viscus friction coefficient	0.022 $Vs/rad$
$K_{pp}$	Thrust constant of pitch	0.0011 $Nm/V$
$K_{py}$	Relative pitch-yaw thrust constant	0.0021 $Nm/V$
$K_{yy}$	Relative yaw-pitch thrust constant	-0.0027 $Nm/V$
$K_{yy}$	Thrust constant of yaw	0.002 $Nm/V$
$m$	Mass of body	1.075 $Kg$
$l$	distance from the center of mass to rotation point	0.0071 $m$
$g$	Gravitational Acceleration	9.81 $m/s^2$

## 2.2 T-S Fuzzy Model

This is a rule-based method of representation for nonlinear systems with fuzzy antecedents and local linear input-output models in the consequent, as shown in Equation (3):

*Rule i:* IF  $v_1(t)$  is  $M_1^i$  AND ... AND  $v_p(t)$  is  $M_p^i$   
THEN  $\dot{x}(t) = A_i x(t) + B_i u(t)$  (3)

Where,  $M_j^i$  is fuzzy set,  $j = 1, 2, \dots, p$  with  $p$  denoting total number of premise variables,  $v(t) = [v_1(t) \ v_2(t) \ \dots \ v_p(t)] \in R^p$  is premise vector,  $i = 1, 2, \dots, l$  with  $l$  denoting total number of model rules,  $x(t) \in R^n$  is state vector,  $u(t) \in R^m$  is input vector,  $A_i \in R^{n \times n}$ ,  $B_i \in R^{n \times m}$ . The fuzzy system output in crisp form is given as:

$$\dot{x}(t) = \sum_{i=1}^l J_i(v(t)) [A_i x(t) + B_i u(t)] \quad (4)$$

Where

$$\sum_{i=1}^l J_i(v(t)) = 1,$$

$$J_i(v(t)) = \frac{\prod_{j=1}^p M_{ij}(v_j(t))}{\sum_{i=1}^l \prod_{j=1}^p M_{ij}(v_j(t))} \geq 0 \ \forall i.$$

$J_i(v(t))$  is the normalized grade of membership,  $M_{ij}(v_j(t))$  is grade of membership of  $v_j(t)$  for fuzzy set  $M_{ij}$ . In the rest of the paper, for simplicity  $J_i(v) = J_i(v(t))$  will be used and  $(t)$  will be omitted.

## 2.3 Fuzzy Controller

It uses a set of linear state feedback controllers designed for local linear sub-systems of the respective rule of the fuzzy model given in Equation (4). The  $i^{th}$  fuzzy rule for this controller will be similar to the T-S

fuzzy model; only the consequent part has a state feedback controller, given by Equation (5):

*Rule i:* IF  $v_1$  is  $M_1^i$  AND ... AND  $v_p$  is  $M_p^i$   
THEN  $u_{fuzzy} = -K_i e \quad i = 1, 2, \dots, l$  (5)

Where,  $e \in R^n$  is the error vector and  $K_i \in R^{m \times n}$  is the constant feedback gains matrix for the respective  $i^{th}$  rule. The error vector is defined by the difference between the state vector  $x$  and the desired state vector.

$x_d \in R^n$  as

$$e = x - x_d$$

The fuzzy controller output in crisp form is given in Equation (6):

$$u = - \sum_{i=1}^l J_i(v) K_i e$$

$$u = -\tilde{K} e \quad (6)$$

Where,  $\tilde{K} = \sum_{i=1}^l J_i(v) K_i$ , so it is a fuzzy aggregation of local linear state feedback controllers.

**Lemma 1** [25]: The closed-loop fuzzy system will be asymptotically stable if there exists a positive definite matrix  $P$  such that

$$(A_i - B_i K_i)^T P + P(A_i - B_i K_i) < 0$$

$$\left( \frac{(A_i - B_i K_j) + (A_i - B_j K_i)}{2} \right)^T P$$

$$+ P \left( \frac{(A_i - B_i K_j) + (A_i - B_j K_i)}{2} \right)$$

$$\leq 0 \quad i < j \leq r$$

## 2.4 Fuzzy sliding mode controller

For desired trajectory tracking while rejecting the gravitational disturbance present in pitch dynamics a new fuzzy sliding mode controller is designed in this sub-section. Let's reconsider the 2-DOF aero system, given in Equation (7):

$$\begin{bmatrix} \dot{x}_1 \\ \dot{x}_2 \\ \dot{x}_3 \\ \dot{x}_4 \end{bmatrix} = \begin{bmatrix} x_3 \\ x_4 \\ f_1 \\ f_2 \end{bmatrix} + \begin{bmatrix} 0 & 0 \\ 0 & 0 \\ g_{11} & g_{12} \\ g_{21} & g_{22} \end{bmatrix} \begin{bmatrix} V_p \\ V_y \end{bmatrix} + \begin{bmatrix} 0 \\ 0 \\ d_g \\ 0 \end{bmatrix} \quad (7)$$

Where,  $f_1 = \frac{-B_p x_3 - m l^2 \cos x_1 \sin x_1 x_4^2}{J_p + m l^2}$  is a nonlinear function of states,  $d_g = \frac{-m g l \cos x_1}{J_p + m l^2}$  is considered a disturbance.

**Assumption 1:** The  $d_g$  is a bounded, state-dependent disturbance; its upper bound is  $\epsilon$ , given in Equation (8),

$$\left| \frac{m g l \cos x_1}{J_p + m l^2} \right| \leq \epsilon \quad \forall x_1 \quad (8)$$

**Assumption 2:** The desired trajectories  $x_d = [x_{1d} \ x_{2d} \ x_{3d} \ x_{4d}]^T \in R^4$  are bounded and continuously second-order differentiable  $x_d \in C^2$  and the desired pitch and yaw angular velocities are given as  $[\dot{x}_{3d}, \dot{x}_{4d}] = [\dot{x}_{1d}, \dot{x}_{2d}]$ . The tracking error vector  $e = [e_1, e_2, e_3, e_4]^T = x - x_d = [x_1 - x_{1d}, x_2 - x_{2d}, x_3 - x_{3d}, x_4 - x_{4d}]^T$ . The control objective is that all states should track the desired trajectories, which means the convergence of the error vector  $e$  to zero as time increases from zero to infinity.

$$e \rightarrow 0 \text{ as } t \rightarrow \infty$$

$$x \rightarrow x_d \text{ as } t \rightarrow \infty$$

The integral sliding surface  $s = [s_1, s_2]^T \in R^2$  is selected for pitch and yaw angular velocity to overcome the gravitational pitch disturbance as:

$$s(t) = \begin{bmatrix} s_1(t) \\ s_2(t) \end{bmatrix} = \begin{bmatrix} e_3(t) \\ e_4(t) \end{bmatrix} - \begin{bmatrix} e_3(0) \\ e_4(0) \end{bmatrix} - \int_0^t \begin{bmatrix} \dot{e}_3(e, u_{fuzzy}, t) \\ \dot{e}_4(e, u_{fuzzy}, t) \end{bmatrix} d\tau \quad (9)$$

Here,  $s(t) \in R^2$  is sliding variable.  $e_3(0)$  &  $e_4(0)$  are the initial value of error, and  $u_{fuzzy} = [V_{pfuzzy}, V_{yfuzzy}]^T \in R^2$  is fuzzy controller output, discussed in the previous section. Substituting the  $\dot{e}_3$  and  $\dot{e}_4$  in Equation (9),

$$s(t) = \begin{bmatrix} s_1(t) \\ s_2(t) \end{bmatrix} = \begin{bmatrix} e_3(t) \\ e_4(t) \end{bmatrix} - \begin{bmatrix} e_3(0) \\ e_4(0) \end{bmatrix} - \int_0^t \left\{ \begin{bmatrix} f_1 \\ f_2 \end{bmatrix} + \begin{bmatrix} g_{11} & g_{12} \\ g_{21} & g_{22} \end{bmatrix} \begin{bmatrix} V_{pfuzzy} \\ V_{yfuzzy} \end{bmatrix} - \begin{bmatrix} \dot{x}_{3d} \\ \dot{x}_{4d} \end{bmatrix} \right\} d\tau \quad (10)$$

The closed-loop system during sliding mode shows both sliding variables  $s_1 = s_2 = 0$ . Therefore, equivalent control is calculated by  $\dot{s} = \dot{s}_1 = \dot{s}_2 = 0$ . Differentiating Equation (10) with respect to time,

$$\dot{s} = \begin{bmatrix} \dot{s}_1 \\ \dot{s}_2 \end{bmatrix} = \begin{bmatrix} \dot{e}_3 \\ \dot{e}_4 \end{bmatrix} - \begin{bmatrix} f_1 \\ f_2 \end{bmatrix} - \begin{bmatrix} g_{11} & g_{12} \\ g_{21} & g_{22} \end{bmatrix} \begin{bmatrix} V_{pfuzzy} \\ V_{yfuzzy} \end{bmatrix} + \begin{bmatrix} \dot{x}_{3d} \\ \dot{x}_{4d} \end{bmatrix} = 0 \quad (11)$$

Substituting the values of  $\dot{e}_3$  and  $\dot{e}_4$  in Equation (11),

$$\begin{bmatrix} \dot{x}_3 - \dot{x}_{3d} \\ \dot{x}_4 - \dot{x}_{4d} \end{bmatrix} - \begin{bmatrix} f_1 \\ f_2 \end{bmatrix} - \begin{bmatrix} g_{11} & g_{12} \\ g_{21} & g_{22} \end{bmatrix} \begin{bmatrix} V_{pfuzzy} \\ V_{yfuzzy} \end{bmatrix} + \begin{bmatrix} \dot{x}_{3d} \\ \dot{x}_{4d} \end{bmatrix} = 0 \quad (12)$$

Substituting the values of  $\dot{x}_3$  and  $\dot{x}_4$  in Equation (12),

$$\begin{bmatrix} f_1 \\ f_2 \end{bmatrix} + \begin{bmatrix} g_{11} & g_{12} \\ g_{21} & g_{22} \end{bmatrix} \begin{bmatrix} V_p \\ V_y \end{bmatrix} + \begin{bmatrix} d_g \\ 0 \end{bmatrix} - \begin{bmatrix} f_1 \\ f_2 \end{bmatrix} - \begin{bmatrix} g_{11} & g_{12} \\ g_{21} & g_{22} \end{bmatrix} \begin{bmatrix} V_{pfuzzy} \\ V_{yfuzzy} \end{bmatrix} = 0 \quad (13)$$

For the calculation of equivalent control, it is assumed that no disturbances are present in the system. So the equivalent control is selected as fuzzy controller output Equation (6) which is given by:

$$\begin{bmatrix} V_{peq} \\ V_{yeq} \end{bmatrix} = \begin{bmatrix} V_{pfuzzy} \\ V_{yfuzzy} \end{bmatrix} \quad (14)$$

Defining a positive definite Lyapunov function as,

$$V = \frac{s^T s}{2} \quad (15)$$

Differentiating the Equation (15) with respect to time,

$$\dot{V} = s^T \dot{s} \quad (16)$$

Substituting the value of  $\dot{s}$  from Equations (13) to (16)

$$\begin{aligned} \dot{V} &= s^T \begin{bmatrix} \dot{s}_1 \\ \dot{s}_2 \end{bmatrix} = s^T \left[ \begin{bmatrix} f_1 \\ f_2 \end{bmatrix} + \begin{bmatrix} g_{11} & g_{12} \\ g_{21} & g_{22} \end{bmatrix} \begin{bmatrix} V_p \\ V_y \end{bmatrix} + \begin{bmatrix} d_g \\ 0 \end{bmatrix} \right. \\ &\quad \left. - \begin{bmatrix} f_1 \\ f_2 \end{bmatrix} - \begin{bmatrix} g_{11} & g_{12} \\ g_{21} & g_{22} \end{bmatrix} \begin{bmatrix} V_{pfuzzy} \\ V_{yfuzzy} \end{bmatrix} \right] \\ \dot{V} &= s^T \left[ \begin{bmatrix} g_{11} & g_{12} \\ g_{21} & g_{22} \end{bmatrix} \begin{bmatrix} V_p \\ V_y \end{bmatrix} + \begin{bmatrix} d_g \\ 0 \end{bmatrix} - \begin{bmatrix} g_{11} & g_{12} \\ g_{21} & g_{22} \end{bmatrix} \begin{bmatrix} V_{pfuzzy} \\ V_{yfuzzy} \end{bmatrix} \right] \end{aligned} \quad (17)$$

The control law of fuzzy sliding mode control is selected as:

$$\begin{aligned} \begin{bmatrix} \dot{V}_p \\ \dot{V}_y \end{bmatrix} &= u_{fuzzy} - \begin{bmatrix} g_{11} & g_{12} \\ g_{21} & g_{22} \end{bmatrix}^{-1} \eta \frac{s}{|s|} \\ \begin{bmatrix} \dot{V}_p \\ \dot{V}_y \end{bmatrix} &= \begin{bmatrix} V_{pfuzzy} \\ V_{yfuzzy} \end{bmatrix} - \begin{bmatrix} g_{11} & g_{12} \\ g_{21} & g_{22} \end{bmatrix}^{-1} \eta \frac{s}{|s|} \end{aligned} \quad (18)$$

Substituting the control law from Equations (17) to (18),

$$\begin{aligned} \dot{V} &= s^T \left[ \begin{bmatrix} g_{11} & g_{12} \\ g_{21} & g_{22} \end{bmatrix} \begin{bmatrix} V_{pfuzzy} \\ V_{yfuzzy} \end{bmatrix} \right. \\ &\quad \left. - \begin{bmatrix} g_{11} & g_{12} \\ g_{21} & g_{22} \end{bmatrix}^{-1} \eta \frac{s}{|s|} \right] + \begin{bmatrix} d_{gu} \\ 0 \end{bmatrix} \\ &\quad - \begin{bmatrix} g_{11} & g_{12} \\ g_{21} & g_{22} \end{bmatrix} \begin{bmatrix} V_{pfuzzy} \\ V_{yfuzzy} \end{bmatrix} \\ \dot{V} &= s^T \left[ -\eta \frac{s}{|s|} + \begin{bmatrix} d_{gu} \\ 0 \end{bmatrix} \right] \\ \dot{V} &= -\eta \frac{s^T s}{|s|} + s^T \begin{bmatrix} d_{gu} \\ 0 \end{bmatrix} \\ \dot{V} &= -\eta |s| + s^T \begin{bmatrix} d_{gu} \\ 0 \end{bmatrix} \end{aligned} \quad (19)$$

Where  $\eta = \text{diag}(\eta_1, \eta_2) > \epsilon$ . The Equation (19) may be expressed as:

$$\dot{V} \leq -\eta |s| + |s| |d_g| \quad (20)$$

Equation (20) demonstrates that the closed-loop system will be asymptotically stable. The Lyapunov variable  $V$  and sliding variable  $s$  will converge to zero as time increases to infinity.

## 2.5 Application

The fuzzy controller explained in the previous subsection is a model-based controller design approach, so the local approximation method was employed to create the T-S fuzzy model for the 2-DOF aero system. The dynamics of the 2-DOF aero system mostly depend on the pitch angle so five operating points for pitch angle,  $x_1 = [-\pi/4, -\pi/8, 0, +\pi/8, +\pi/4]$  rad, and remaining states  $[x_2, x_3, x_4]^T = [0, 0, 0]^T$  were selected. Around these five operating points, triangular and trapezoidal membership functions were employed for this fuzzy model. The membership functions were uniformly distributed and covered the

entire operating range. Figure 2 illustrates the membership function of the state  $x_1$ .

The system (2) has been linearized for these operating points and the linearized model of the aero system is given in Appendix I. T-S Fuzzy model's fuzzy rules are given in Table 2.

For each linear sub-system of aero, an LQR controller has been designed. The Q and R matrices are selected as:

$$Q = \text{diag}(150, 150, 200, 200), R = \text{diag}(1, 1)$$

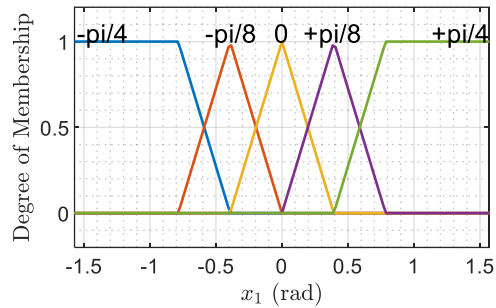


Figure 2: Membership functions of state  $x_1$ .

Table 2: Rule Base of Fuzzy model.

Rule	Condition
Rule 1	IF $x_1$ is $-\pi/4$ THEN $\dot{x} = A_1x + B_1u$
Rule 2	IF $x_1$ is $-\pi/8$ THEN $\dot{x} = A_2x + B_2u$
Rule 3	IF $x_1$ is 0 THEN $\dot{x} = A_3x + B_3u$
Rule 4	IF $x_1$ is $+\pi/8$ THEN $\dot{x} = A_4x + B_4u$
Rule 5	IF $x_1$ is $+\pi/4$ THEN $\dot{x} = A_5x + B_5u$

Where,

$$\begin{aligned} A_1 &= \begin{bmatrix} 0 & 0 & 1 & 0 \\ 0 & 0 & 0 & 1 \\ -2.4116 & 0 & -0.32239 & 0 \\ 0 & 0 & 0 & -0.9988 \end{bmatrix} \\ A_2 &= \begin{bmatrix} 0 & 0 & 1 & 0 \\ 0 & 0 & 0 & 1 \\ -1.3051 & 0 & -0.32239 & 0 \\ 0 & 0 & 0 & -0.9988 \end{bmatrix} \\ A_3 &= \begin{bmatrix} 0 & 0 & 1 & 0 \\ 0 & 0 & 0 & 1 \\ 0 & 0 & -0.32239 & 0 \\ 0 & 0 & 0 & -0.9988 \end{bmatrix} \\ A_4 &= \begin{bmatrix} 0 & 0 & 1 & 0 \\ 0 & 0 & 0 & 1 \\ 1.3051 & 0 & -0.32239 & 0 \\ 0 & 0 & 0 & -0.9988 \end{bmatrix} \end{aligned}$$

$$A_5 = \begin{bmatrix} 0 & 0 & 1 & 0 \\ 0 & 0 & 0 & 1 \\ 2.4116 & 0 & -0.32239 & 0 \\ 0 & 0 & 0 & -0.9988 \end{bmatrix}$$

$$B_1 = B_2 = B_3 = B_4 = B_5 = \begin{bmatrix} 0 & 0 \\ 0 & 0 \\ 0.5010 & 0.0957 \\ -0.1226 & 0.9990 \end{bmatrix}$$

The feedback gain matrix of LQR controllers is obtained as:

$$K_1 = \begin{bmatrix} 0.7067 & -9.9442 & 7.1980 & -10.999 \\ 3.3390 & 7.1494 & 11.1679 & 7.9108 \\ 2.1623 & -10.0404 & 7.9186 & -11.101 \\ 4.6875 & 7.0135 & 12.0082 & 7.7735 \\ 6.7070 & -10.2477 & 10.0278 & -11.347 \end{bmatrix}$$

$$K_2 = \begin{bmatrix} 10.2477 & 6.7070 & 14.8478 & 7.4611 \\ 16.7396 & -10.5003 & 13.7825 & -11.580 \\ 24.4661 & 6.3042 & 20.4479 & 7.0366 \\ 27.1666 & -10.6523 & 16.8831 & -11.742 \\ 40.1751 & 6.0439 & 25.3475 & 6.7539 \end{bmatrix}$$

By using these feedback gain matrices, the fuzzy controller using the T-S fuzzy model has been designed. Fuzzy controller rules are given in Table 3.

**Table 3:** Rule base of fuzzy controller.

Rule	Condition
<b>Rule 1</b>	IF $e_1$ is $-\pi/4$ THEN $u_{fuzzy} = -K_1 e$
<b>Rule 2</b>	IF $e_1$ is $-\pi/8$ THEN $u_{fuzzy} = -K_2 e$
<b>Rule 3</b>	IF $e_1$ is 0 THEN $u_{fuzzy} = -K_3 e$
<b>Rule 4</b>	IF $e_1$ is $+\pi/8$ THEN $u_{fuzzy} = -K_4 e$
<b>Rule 5</b>	IF $e_1$ is $+\pi/4$ THEN $u_{fuzzy} = -K_5 e$

In the fuzzy controller, the antecedent part of fuzzy rules will be the same as the T-S fuzzy model but the consequent part contains an LQR controller. The weighted average method was employed to obtain the defuzzified output, given in Equation (21):

$$u_{fuzzy} = - \sum_{i=1}^5 J_i(v) K_i e = -\tilde{K} e \quad (21)$$

Using linear matrix inequality, the common positive definite matrix  $P$  for the asymptotic stability of the closed-loop fuzzy system is determined and given in Equation (22) as follows:

$$P = \begin{bmatrix} 17.6835 & -0.3999 & 3.4268 & -0.3768 \\ -0.3999 & 22.2840 & -0.5590 & 4.5500 \\ 3.4268 & -0.5590 & 4.4538 & -0.5210 \\ -0.3768 & 4.5500 & -0.5210 & 4.2601 \end{bmatrix} \quad (22)$$

The proposed fuzzy sliding mode controller for 2-DOF aero system is given in Equation (23) as:

$$\begin{bmatrix} \dot{V}_p \\ \dot{V}_y \end{bmatrix} = u_{fuzzy} - \begin{bmatrix} g_{11} & g_{12} \\ g_{21} & g_{22} \end{bmatrix}^{-1} \eta \frac{s}{|s|+\delta} \quad (23)$$

Here  $\eta_1, \eta_2 = 5$ ,  $\delta = 0.01$ . the  $\delta$  is used to minimize the chattering. These parameters are selected by asymptotic convergence conditions shown in Equation (20).

### 3 Results and Discussions

This section evaluates the effectiveness of previously designed FC and FSMC for the 2-DOF aero system using parameters given in Table 1. An LQR controller [21] was designed for operating points [0,0,0,0,0] and the integration of both outputs is selected as two additional states. A robust backstepping controller (BS) [3] was also designed for comparison with other controllers. All controllers have been implemented on MATLAB Simulink. The fixed sample time of 0.001 seconds was used in the simulation.

#### 3.1 Case 1: Stabilization

Fig. 3 demonstrates the performance of LQR, BS, FC, and FSMC for stabilization of initial conditions. The initial conditions of the system are selected as [40° 45° 0 0].

Figure 3(a) and (b) show that both pitch and yaw angles are converging to zero in some finite time. The LQR controller was designed for a smaller operating range of about  $\pm 10^\circ$  pitch angles. So, when the initial condition is situated beyond this range, its performance is degraded. The FC settles around  $-13.2^\circ$  due to an uncompensated gravitational pitch disturbance. The FSMC-based system stabilizes the states in less time as compared to the FC and LQR controllers. Figure 3 (c) and (d) show the pitch and yaw angular velocities of the system with all controllers. Both velocities also converged to zero as pitch and yaw angles converged to zero. Figure 3(e) and (f) show the output of all controllers, pitch, and yaw motor voltages. Table 4 lists the stabilization parameters of the transient and steady-state response. In Table 4,  $t_s$  stands for settling time,  $e_{ss}$  stands for steady-state error. The LQR controller has zero steady-state error, but the settling time is much larger than FC and FSMC, which is 9 seconds in pitch response and 6 seconds in yaw response.

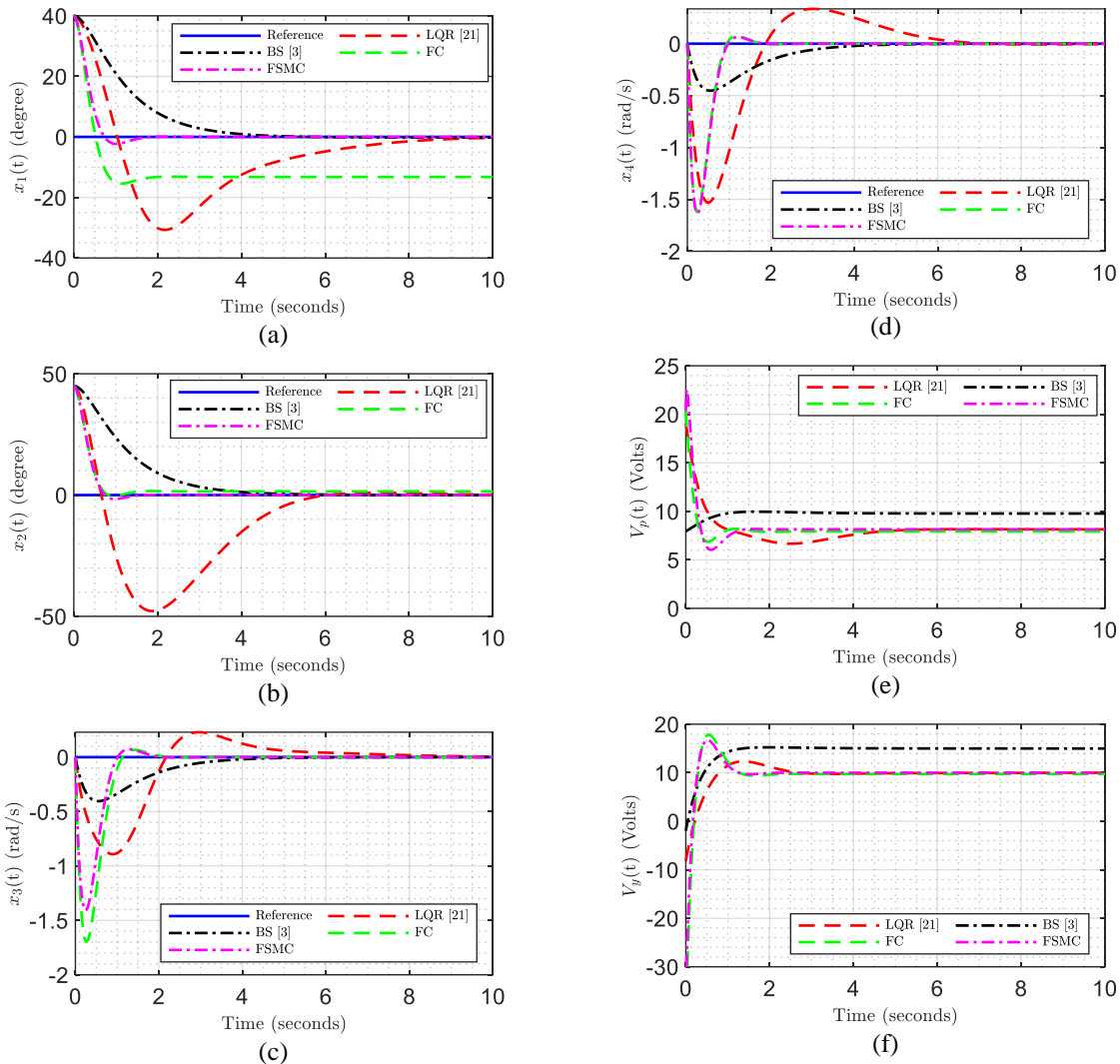


**Figure 3:** Response of (a) pitch angle, (b) yaw angle, (c) pitch angular velocity, (d) yaw angular velocity, (e) input voltage of pitch motor, (f) input voltage of yaw motor.

**Table 4:** Comparison of controllers for steady-state response.

Method	Pitch Response		Yaw Response	
	$t_s$ (s)	$e_{ss}$ (°)	$t_s$ (s)	$e_{ss}$ (°)
LQR [21]	9	0	6	0
BS [3]	3.5	-0.1	3.4	-0.1
FC	1.7	13.2	1.8	1.1
FSMC	1.6	0	1.7	0

The FC shows the largest steady-state error of  $13.2^\circ$  in pitch response but has a small steady-state error of  $1.5^\circ$  in yaw response. The BS shows the overdamped response; it required 3.5 seconds in pitch and 3.4 seconds in yaw response with  $0.1^\circ$  steady-state error. The FSMC required a settling time of 1.6

seconds in pitch response and 1.7 seconds in yaw response, without any steady-state error.

### 3.2 Case 2: Set Point Tracking

To demonstrate the performance of designed controllers for set point tracking, the set points are selected as  $[-20^\circ \ 45^\circ \ 0 \ 0]$  with the initial condition of the system as  $[-40^\circ \ -45^\circ \ 0 \ 0]$ .

All the controller's tracking of pitch angle set point is displayed in Figure 4(a). LQR controller shows the largest settling time as compared to FC and FSMC shows the sluggish response. It also shows a larger overshoot than other controllers. The FC-based

system's pitch angle settles to  $6.5^\circ$  with a large steady-state error of  $13.5^\circ$ . This shows the effect of gravitational pitch disturbance. The FSMC tracks the set point with minimum overshoot, least settling time and no steady-state error present in the response. Figure 4(b) depicts the tracking of each controller's yaw angle set point. The LQR controller tracks the yaw set point with the largest settling time as compared to FC and FSMC. The FC also tracks the yaw set point with a smaller overshoot and lesser steady-state error as compared to the pitch set point.

The FSMC shows lesser overshoot and steady-state error than the FC for the yaw response. Figure 4(c) and (d) show the pitch and yaw angular velocities with all controllers. The angular velocity with FC and FSMC is more than LQR, showing fast-tracking. Figure 4(e) and (f) show the outputs of all controllers. The FC and FSMC have larger control outputs than LQR. Table 5 lists the stabilization parameters of the transient and steady-state response. In Table 5,  $t_s$  stands for settling time,  $M_p$  stands for maximum overshoot,  $e_{ss}$  stands for steady-state error.

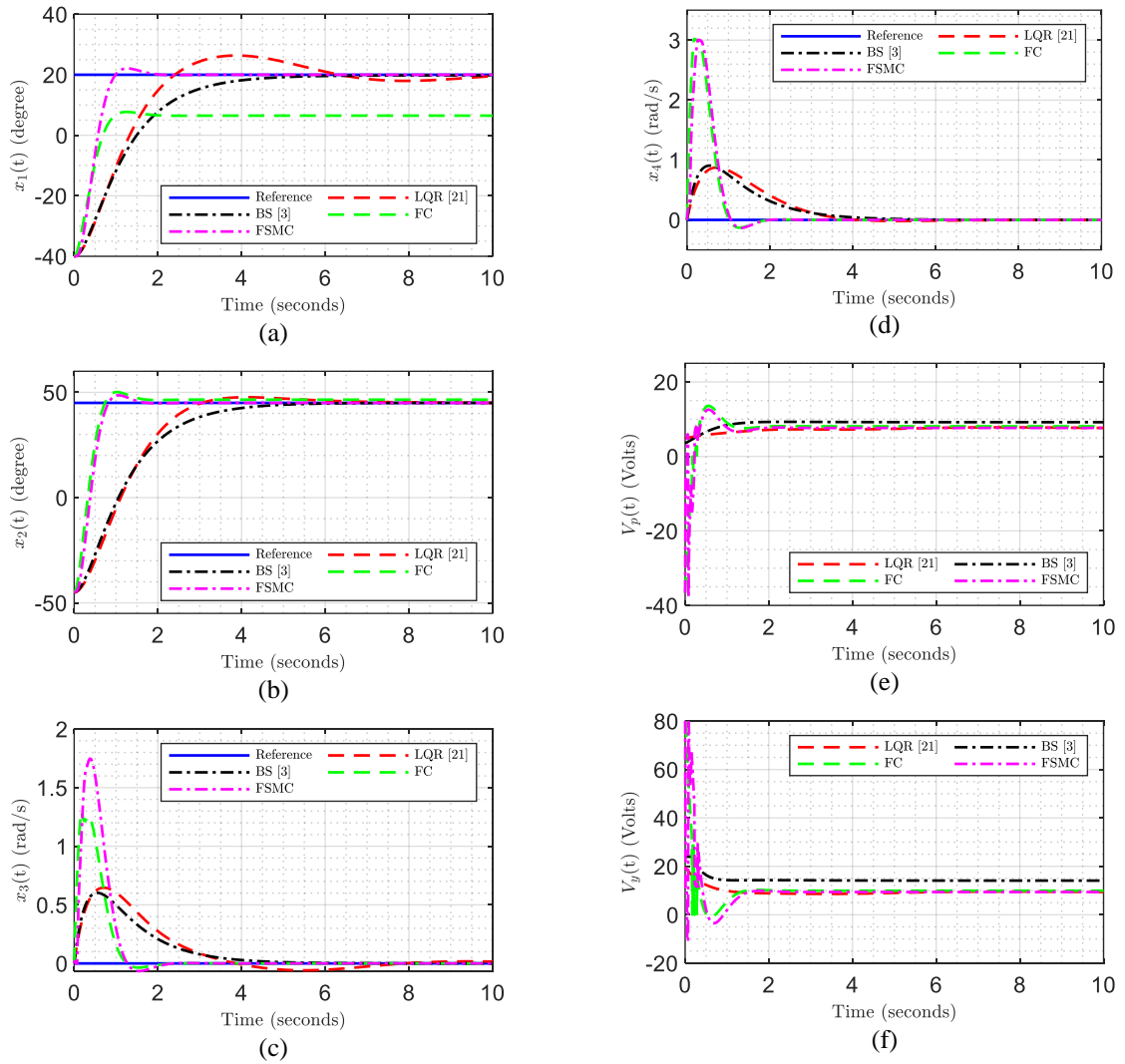


**Figure 4:** Response of (a) pitch angle, (b) yaw angle, (c) pitch angular velocity, (d) yaw angular velocity, (e) input voltage of pitch motor, (f) input voltage of yaw motor.

**Table 5:** Comparison of controllers for transient and steady-state response.

Method	Pitch Response			Yaw Response		
	$t_s$ (s)	$M_p$ (%)	$e_{ss}$ (°)	$t_s$ (s)	$M_p$ (%)	$e_{ss}$ (°)
LQR[21]	13	12.5	0	5.0	-	-0.2
BS [3]	6.0	-	0.2	6.5	-	0.5
FC	2.0	-	13.5	1.8	7.3	-1.5
FSMC	1.7	5	0	1.6	3.3	0

The LQR controller shows a settling time of 13 seconds in pitch angle tracking, but it has a 12.5% overshoot as compared to FC and FSMC. It has no overshoot and  $-0.2^\circ$  steady state error in yaw angle tracking. FC shows less settling time as compared to

LQR, but has a large steady-state error of  $13.5^\circ$  in pitch angle tracking. FC shows an overshoot of 7.3% with 1.8 seconds settling time for yaw set point tracking. The BS shows an overdamped response, so no overshoot is present in the pitch and yaw response, but the settling time is very large as compared to FC and FSMC. A small steady-state error of  $0.2^\circ$  and  $0.5^\circ$  is present in the pitch and yaw response. The FSMC shows minimum overshoot, lesser settling time, and no steady-state error as compared to both FC and LQR. It required 1.7 seconds to track the pitch set point with a 5% overshoot with zero steady-state error. For yaw set point tracking, it required 1.6 seconds with 3.33% overshoot and no steady-state error.

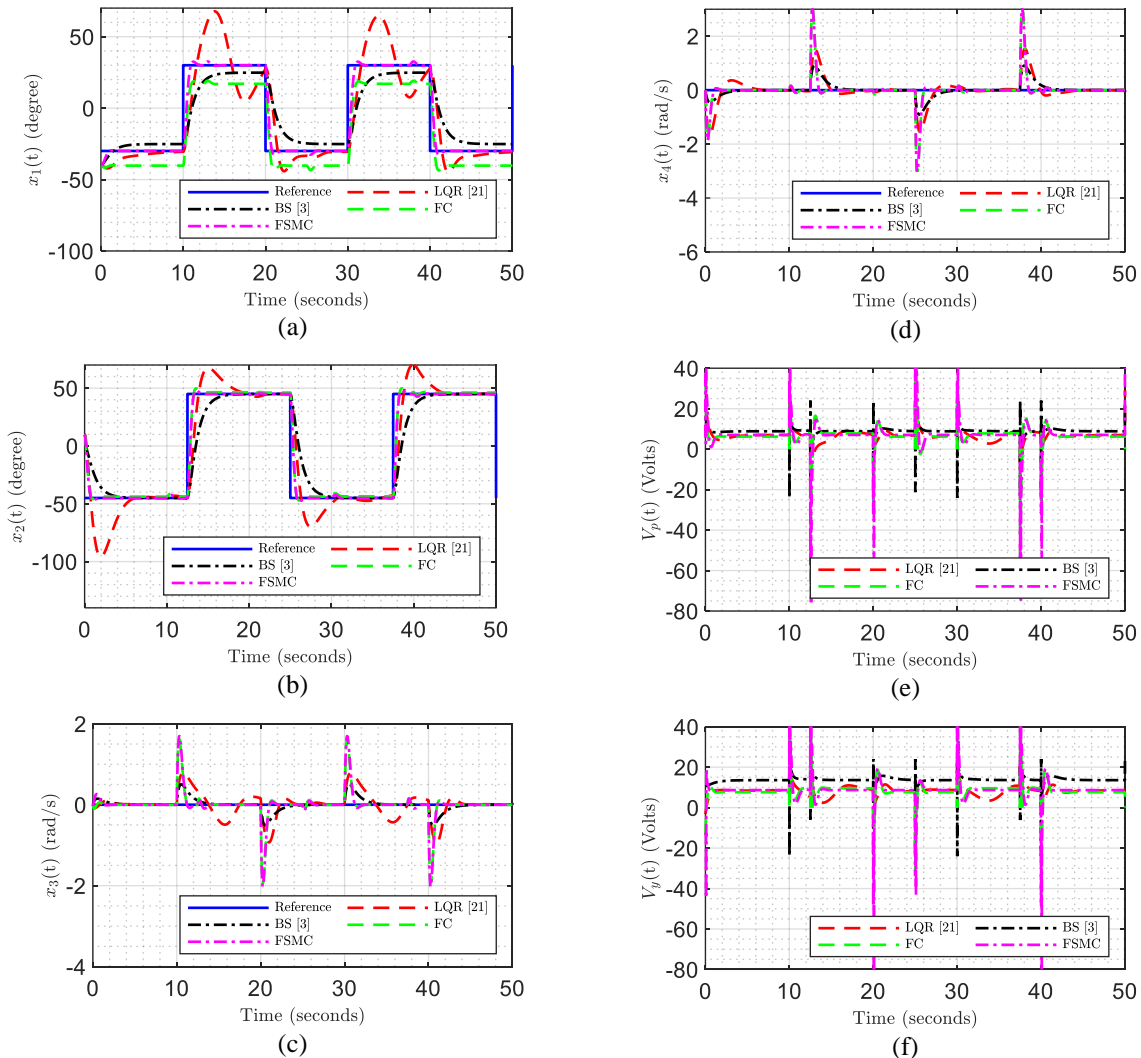


**Figure 5:** Response of (a) pitch angle, (b) yaw angle, (c) pitch angular velocity, (d) yaw angular velocity, (e) input voltage of pitch motor, (f) input voltage of yaw motor.

### 3.3 Case 3: Square wave trajectory tracking

To evaluate the responsiveness and robustness of the proposed controller, square wave trajectories have been selected as the reference. This trajectory changes its value abruptly, introducing a tracking error in the system. This shows the ability of the system to respond to discontinuous inputs or quickly changing inputs. Figure 5 illustrates the tracking of the desired square wave trajectory for a greater pitch angle of 25 square( $2\pi t/20$ ) and yaw as 45 square( $2\pi t/25$ ) (in degrees) with initial conditions as  $[-40^\circ 0^\circ 0 0]$ .

Figure 5(a) depicts the pitch angular position response of all controllers. LQR has a large overshoot and settling time for this trajectory as compared to the previous square trajectory. Here, the trajectory is beyond the operating range of the LQR controller, so it shows more oscillations and a larger settling time. FC shows the tracking of the trajectory with a constant tracking error due to gravitational disturbance. BS shows the overdamped response, so the settling time is larger. FSMC easily tracks the trajectory with an overshoot and a shorter settling time. Figure 5(b) depicts the response of the yaw angle for a square wave trajectory.

All controllers are tracking the square yaw trajectory. LQR has the largest settling time and overshoot. FC and FSMC show similar responses. BS shows an overdamped response. Figure 5(c) and (d) depict the pitch and yaw angular velocity response. Figure 5(e) and (f) show the controllers' outputs.

**Table 6:** Comparison of controllers for the transient response of different square wave trajectories.

Trajectory		Method	Pitch Response	
A (°)	f (Hz)		$t_s$ (s)	$M_p$ (%)
5	0.025	LQR[21]	7	-
		BS [3]	5	-
		FC	2	-
		FSMC	1.7	5
15	0.025	LQR[21]	10	8.67
		BS [3]	5	-
		FC	2	-
		FSMC	1.7	5
25	0.025	LQR[21]	16	23.2
		BS [3]	5	-
		FC	2	-
		FSMC	1.7	5

Table 6 shows the transient response of square wave pitch trajectory tracking of three different amplitudes and the same frequency. The settling time and maximum overshoot of the LQR controller change with reference trajectory amplitude. The LQR is a linear controller, so its operating range is less. As the operating range increases, its performance changes. The FC, BS, and FSMC are nonlinear controllers and have larger operating ranges, so their responses are similar for all cases.

### 3.4 Case 4: Sinusoidal trajectory tracking

To assess the ability of the proposed controller for time-varying inputs, sinusoidal trajectories have been selected as the reference.

This trajectory changes its value at each instance of time. For this case, two sinusoidal trajectories are selected as  $30 \sin(2\pi t/20)$  and  $45 \sin(2\pi t/25)$  (in degrees) for pitch and yaw, respectively. The initial condition of the system for this case is selected as  $[40^\circ 0^\circ 0 0]$ .

Figure 6(a) depicts the pitch angular position with sine wave trajectory for all controllers. The LQR has a poor response for time-varying trajectories. FC is tracking the trajectory with a constant tracking error. FSMC easily tracks the trajectory with less settling time. BS tracks the trajectory with a small steady-state error as compared to FSMC. Figure 6(b) depicts the yaw angular position with a sine wave trajectory for all controllers. LQR tracks the sine wave trajectory for lower angular positions, but when the angular position changes after 20, its performance degrades due to a smaller operating range. This response shows the largest settling time with steady-state error. FC, BS, and FSMC have similar responses, and both are tracking the desired yaw trajectory. Figure 6(c) and (d) depict the tracking of desired pitch and yaw angular velocity. FC, BS, and FSMC are tracking the desired angular velocity trajectories. Figure 6(e) and (f) show the controller outputs for sine wave trajectory tracking.

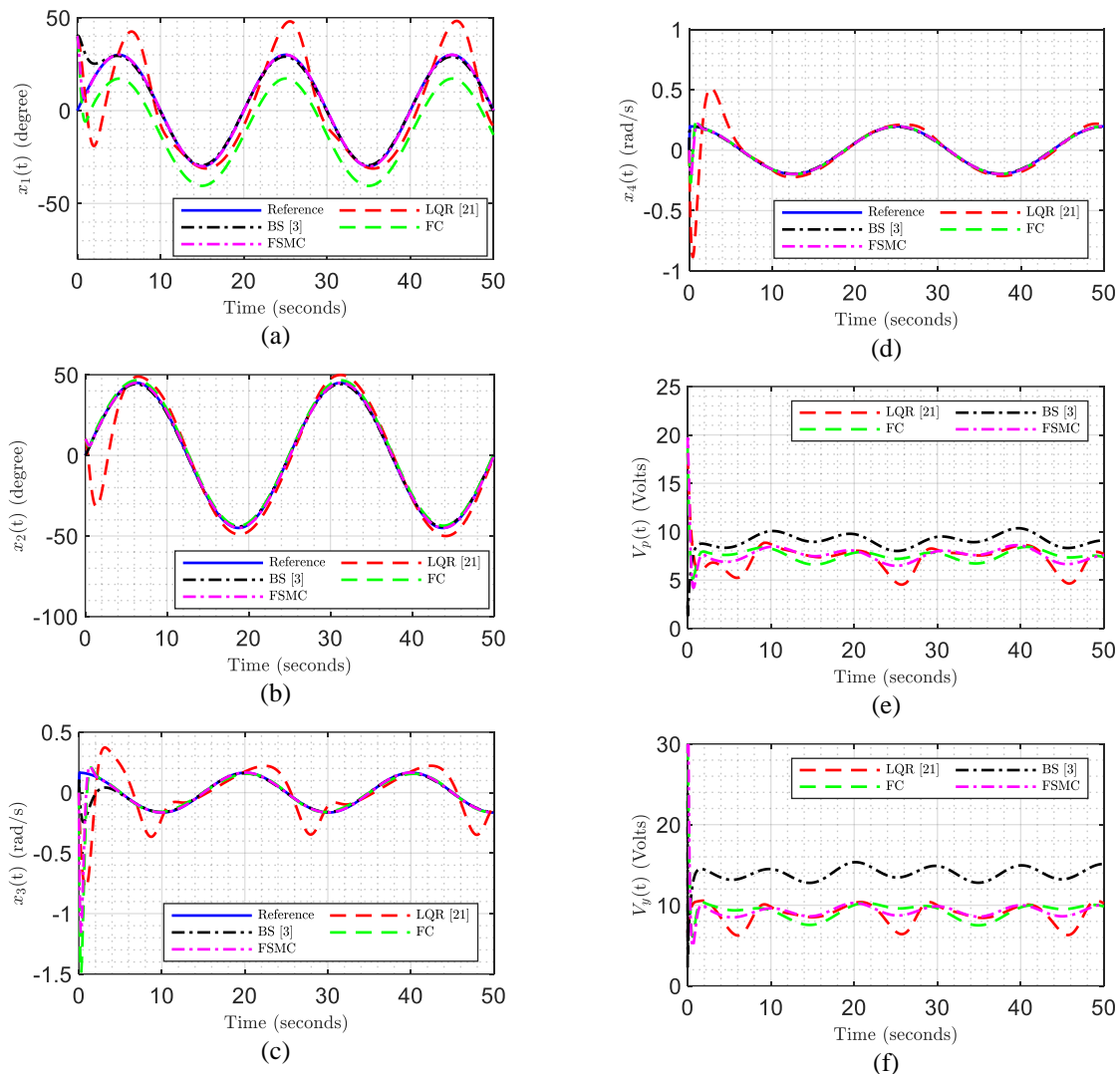


**Figure 6:** Response of (a) pitch angle, (b) yaw angle, (c) pitch angular velocity, (d) yaw angular velocity, (e) input voltage of pitch motor, (f) input voltage of yaw motor.

**Table 7:** Comparison of controllers for IAE, ISE, and ITAE.

Method	IAE		ISE		ITAE	
	Pitch	Yaw	Pitch	Yaw	Pitch	Yaw
LQR [21]	7.18	4.69	1.93	1.14	155.1	77.94
BS [3]	1.45	1.53	0.40	0.5099	14.36	13.54
FC	11.03	1.26	2.49	0.034	273.9	30.89
FSCM	0.37	0.34	0.12	0.0031	3.07	8.25

To evaluate the performance of controllers, three standard performance integral absolute tracking error (IAE), integral square tracking error (ISE), and integral time absolute tracking error (ITAE) for all designed controllers have been used. IAE shows the total absolute error over time and provides a measure

of tracking performance. ISE highlights the larger tracking error more effectively by squaring and shows the impact of deviations. ITAE emphasizes long-duration error with a time-weighted factor, providing the effect of steady-state error and larger settling time. The values of these performance indices are given in Table 7.

The proposed controller has the lowest IAE, ISE, and ITAE for pitch and yaw trajectories. The FC controller always shows tracking errors due to gravitational disturbance in pitch dynamics, so it has the largest value of IAE, ISE, and ITAE in pitch tracking. The LQR controller shows the largest tracking error in yaw trajectory as compared to BS,

FC, and FSMC, due to its limited operating range, it is not able to track the trajectory after  $\pm 15^\circ$ . The BS shows lesser IAE, ISE, and ITAE than FC and LQR, but greater than FSMC due to an overdamped response. The designed FSMC easily tracks both pitch and yaw trajectory with the lowest value of IAE, ISE, and ITAE as compared to other controllers.

#### 4 Conclusions

The work proposed, the design and implementation of a new fuzzy sliding mode controller for the 2-DOF Aero flight control simulator to improve the tracking performance of both pitch and yaw angle trajectories, while gravitational disturbance is present in the system. The previously designed LQR controller [21] helps in tracking pitch and yaw trajectory, but has the largest overshoot and settling time with a greater number of oscillations in pitch response. The robust nonlinear BS controller [3] shows tracking of the desired trajectory, but shows a larger settling time and small steady-state error due to an overdamped response.

The T-S fuzzy model is utilized to construct a fuzzy controller employing the parallel distributed compensation approach. This fuzzy controller is not able to compensate for the gravitational pitch disturbance. The fuzzy controller shows a wide operating range, but the largest tracking error in pitch trajectory is due to gravitational disturbance. The suggested fuzzy sliding mode controller compensates for gravitational disturbance by combining fuzzy and sliding mode controllers. Fixed and time-varying trajectories of trajectories are applied to the system, and the performance of all controllers was compared in terms of IAE, ISE, and ITAE values of tracking error. The simulation study demonstrates that the proposed fuzzy sliding mode controller shows the lowest tracking error, robustness with gravitational disturbance, and a lesser settling time as compared to the LQR and BS controllers.

The future research directions include the implementation of Hardware-in-the-loop (HIL) testing to validate the performance of the designed controller in real-time operating conditions. Additionally, Model Reference Adaptive Control (MRAC) could integrate and enhance the robustness against uncertainty and external disturbance by enabling the controller to adjust its parameters in real-time based on a reference model. The controller provides optimal performance when the system changes its parameters over time. Finally, the

proposed controller could be applied to more complex systems such as unmanned aerial vehicles (UAVs) or real flight platforms, which demonstrate the practicality and application of this controller.

#### Appendix-I

The linear model of the system is required for designing linear state feedback controllers. The Taylor series method [28] for the linearization of nonlinear systems provides the linear model:

$$\dot{x} = f(x_e, u_e) + A(x, u)|_{x_e, u_e}(x - x_e) + B(x, u)|_{x_e, u_e}(u - u_e)$$

and

$$A = \begin{bmatrix} \frac{\partial x_3}{\partial x_1} & \frac{\partial x_3}{\partial x_2} & \frac{\partial x_3}{\partial x_3} & \frac{\partial x_3}{\partial x_4} \\ \frac{\partial x_4}{\partial x_1} & \frac{\partial x_4}{\partial x_2} & \frac{\partial x_4}{\partial x_3} & \frac{\partial x_4}{\partial x_4} \\ \frac{\partial f_1}{\partial x_1} & \frac{\partial f_1}{\partial x_2} & \frac{\partial f_1}{\partial x_3} & \frac{\partial f_1}{\partial x_4} \\ \frac{\partial f_2}{\partial x_1} & \frac{\partial f_2}{\partial x_2} & \frac{\partial f_2}{\partial x_3} & \frac{\partial f_2}{\partial x_4} \end{bmatrix}_{x_{1e}, x_{2e}, x_{3e}, x_{4e}}$$

$$B = \begin{bmatrix} 0 & 0 \\ 0 & 0 \\ \frac{\partial g_{11}}{\partial V_p} & \frac{\partial g_{12}}{\partial V_y} \\ \frac{\partial g_{21}}{\partial V_p} & \frac{\partial g_{22}}{\partial V_y} \end{bmatrix}_{x_{1e}, x_{2e}, x_{3e}, x_{4e}}$$

$$\text{Where, } \frac{\partial f_1}{\partial x_1} = \frac{-ml^2 \cos 2x_{1e} x_{4e}^2 + mgl \sin x_{1e}}{J_p + ml^2}, \quad \frac{\partial f_1}{\partial x_3} = \frac{-B_p}{J_p + ml^2},$$

$$\frac{\partial f_1}{\partial x_4} = \frac{-2ml^2 x_{4e} \cos x_{1e} \sin x_{1e}}{J_p + ml^2}, \quad \frac{\partial f_2}{\partial x_1} =$$

$$\frac{2ml^2 \cos 2x_{1e} x_{3e} x_{4e}}{J_y + ml^2 \cos^2 x_{1e}} + \frac{(-B_y x_4 + 2ml^2 \cos x_{1e} \sin x_{1e} x_{3e} x_{4e})(2ml^2 \cos x_{1e} \sin x_{1e})}{(J_y + ml^2 \cos^2 x_{1e})^2},$$

$$\frac{\partial f_2}{\partial x_3} = \frac{2ml^2 \cos x_{1e} \sin x_{1e} x_{4e}}{J_y + ml^2 \cos^2 x_{1e}}, \quad \frac{\partial f_2}{\partial x_4} =$$

$$\frac{-B_y + 2ml^2 \cos x_{1e} \sin x_{1e} x_{3e}}{J_y + ml^2 \cos^2 x_{1e}}, \quad \frac{\partial f_1}{\partial x_2} = \frac{\partial f_2}{\partial x_2} = 0, \quad \frac{\partial g_{11}}{\partial v_p} =$$

$$\frac{K_{pp}}{J_p + ml^2}, \quad \frac{\partial g_{12}}{\partial v_y} = \frac{K_{py}}{J_p + ml^2}, \quad \frac{\partial g_{21}}{\partial v_p} = \frac{K_{yp}}{J_y + ml^2 \cos^2 x_{1e}}, \quad \frac{\partial g_{22}}{\partial v_y} =$$

$$\frac{K_{yy}}{J_y + ml^2 \cos^2 x_{1e}}.$$

By substituting the required operating points, different linearized models can be obtained.

## Author Contributions

G.K.: conceptualization, methodology, investigation, writing an original draft; N.K.G.: methodology, investigation, reviewing and editing, supervision; J.V.: writing—reviewing and editing. All authors have read and agreed to the published version of the manuscript.

## Conflicts of Interest

The authors declare no conflict of interest.

## References

- [1] A. Boubakir, O. Aissa, A. Pasteur, and H. Badi, “Design and experimentation of a self-tuning PID control applied to the 3DOF helicopter,” *Archives of Control Sciences*, vol. 23, no. 3, pp. 311–331, 2013.
- [2] A. Chaudhary, “Trajectory tracking of a 2-DOF helicopter system using fuzzy controller approach,” in *2021 International Conference on Emerging Techniques in Computational Intelligence*, 2021, pp. 159–164.
- [3] S. Schlanbusch and J. Zhou, “Adaptive backstepping control of a 2-DOF helicopter,” in *2019 7th International Conference on Control, Mechatronics and Automation*, 2019, pp. 210–215.
- [4] S. Kumar, “Set-point tracking of quanser AERO using SMC in the presence of uncertainties,” in *2021 5th International Conference on Intelligent Computing and Control Systems*, 2021, pp. 1595–1601.
- [5] K. R. Palepogu and S. Mahapatra, “Synchronous pitch and yaw orientation control of a twin rotor MIMO system using state varying gain sliding mode control,” *Arabian Journal for Science and Engineering*, vol. 49, no. 12, pp. 16169–16182, 2024.
- [6] B. A. Kumar, S. Gayathri, S. Surendhar, S. Senthilrani, and R. Jeyabharathi, “Robust H-infinity controller for two degree of freedom,” in *2019 IEEE International Conference on System, Computation, Automation and Networking*, 2019, pp. 1–5.
- [7] A. C. Aras and O. Kaynak, “Trajectory tracking of a 2-DOF helicopter system using neuro-fuzzy system with parameterized conjunctors,” in *2014 IEEE/ASME International Conference on Advanced Intelligent Mechatronics*, 2014, pp. 322–326.
- [8] R. Coban, “Adaptive backstepping sliding mode control with tuning functions for nonlinear uncertain systems,” *International Journal of Systems Science*, vol. 50, no. 8, pp. 1517–1529, 2019.
- [9] W. Zhou, C. Liao, and L. Zheng, “Adaptive backstepping control for a class of uncertain nonaffine nonlinear time-varying delay systems with unknown dead-zone nonlinearity,” *Abstract and Applied Analysis*, vol. 2014, pp. 1–14, 2014.
- [10] W. Min, and Q. Liu, “An improved adaptive fuzzy backstepping control for nonlinear mechanical systems with mismatched uncertainties,” *Journal for Control, Measurement, Electronics, Computing and Communications*, vol. 60, no. 1, pp. 1–10, 2019.
- [11] J. Zhu and K. Khayati, “Adaptive sliding mode control – convergence and gain boundedness revisited,” *International Journal of Control*, vol. 89, no. 4, pp. 801–814, 2015.
- [12] S. Roy, S. B. Roy, J. Lee, and S. Member, “Overcoming the underestimation and overestimation problems in adaptive sliding mode control,” *IEEE/ASME Transactions on Mechatronics*, vol. 24, no. 5, pp. 2031–2039, Oct. 2019.
- [13] T. A. Mahmoud, M. E. Belal, and A. R. Shalaby, “Fractional-order fuzzy sliding mode control of uncertain nonlinear MIMO systems using fractional-order reinforcement learning,” *Complex and Intelligent Systems*, vol. 10, no. 2, pp. 3057–3085, 2024.
- [14] S. G. Vijay kumar singh, shyam kamal, Ankit Sanchan, “Prescribed time adaptive constraint control of an uncertain nonlinear 2-DOF helicopter,” *IFAC-PapersOnLine*, vol. 56, no. 2, pp. 6877–6882, 2023.
- [15] S. M. Schlanbusch and J. Zhou, “Adaptive quantized control of uncertain nonlinear rigid body systems,” *Systems & Control Letters*, vol. 175, 2023, Art. no. 105513.
- [16] F. Gopmandal and A. Ghosh, “LQR-based MIMO PID control of a 2-DOF helicopter system with uncertain cross-coupled gain,” *International Federation of Automatic Control – Papers OnLine*, vol. 55, no. 22, pp. 183–188, 2022.
- [17] M. Öztürk and İ. Özkol, “Comparison of self-tuned Neuro - Fuzzy controllers on 2 DOF helicopter: An application,” *SN Applied Sciences*, vol. 3, 2021, Art. no. 124,
- [18] T. Zhang, B. Zhu, L. Zhang, Q. Zhang, and T.

- Hu, "Time-varying uncertainty and disturbance estimator without velocity measurements: Design and application," *Control Engineering Practice*, vol. 143, 2024, Art. no. 105780.
- [19] J. Zhang, Y. Yang, and Z. Zhao, "Adaptive neural network control of a 2-DOF helicopter system with input saturation," *International Journal of Control, Automation and Systems*, vol. 21, no. 1, pp. 318–327, 2023.
- [20] R. Fellag and M. Belhocine, "2-DOF helicopter control via state feedback and full / reduced-order observers," in *2024 2nd International Conference on Electrical Engineering and Automatic Control*, 2024, pp. 1–6.
- [21] E. V. Kumar, G. S. Raaja, and J. Jerome, "Adaptive PSO for optimal LQR tracking control of 2 DoF laboratory helicopter," *Applied Soft Computing*, vol. 41, pp. 1–14, 2015.
- [22] R. Ganapathy and V. Kumar, "Robust MRAC augmented baseline LQR for tracking control of 2 DoF helicopter," *Robotics and Autonomous Systems*, vol. 86, pp. 70–77, 2016.
- [23] T. Y. Chun, J. B. Park, and Y. H. Choi, "Reinforcement Q-learning based on Multirate Generalized Policy Iteration and Its Application to a 2-DOF Helicopter," *International Journal of Control, Automation and Systems*, vol. 16, no. 1, pp. 377–386, 2018.
- [24] S. I. Abdelmaksoud, M. Mailah, and A. M. Abdallah, "Practical real-time implementation of a disturbance rejection control scheme for a twin-rotor helicopter system using intelligent active force control," *IEEE Access*, vol. 9, pp. 4886–4901, 2021.
- [25] H. O. Wang, K. Tanaka, and M. Griffin, "Parallel distributed compensation of nonlinear systems by Takagi-Sugeno fuzzy model," in *Proceedings of 1995 IEEE International Conference on Fuzzy Systems*, 1995, vol. 2, pp. 531–538.
- [26] O. Eray and S. Tokat, "Interval type-2 sliding mode fuzzy controller with a time-varying sliding surface," in *2017 International Conference on Computer Science and Engineering*, 2017, pp. 866–871.
- [27] Z. Yongsheng, L. Zhifeng, C. Ligang, and Y. Wentong, "Enhanced Fuzzy Sliding Mode Controller for a 3-DOF Parallel Link Manipulator," in *2010 2nd International Asia Conference on Informatics in Control, Automation and Robotics*, 2010, pp. 167–172.
- [28] F. Castillo, S. Member, G. Sánchez, and A. N. Model, "2DOF Helicopter Models: A simulation evaluation for MPC applications," in *2017 IEEE 3rd Colombian Conference on Automatic Control*, 2017, pp. 1–6.